

$O_2(^3\Sigma)$ and $O_2(^1\Delta)$ processes in microheterogeneous systems

Eduardo Lissi and María A. Rubio

Departamento de Química, Facultad de Ciencias, Universidad de Santiago de Chile, Casilla 5659, Correo 2, Santiago, Chile.

Abstract- The deactivation of excited pyrene derivatives by $O_2(^3\Sigma)$ and the bleaching of 9-substituted anthracene derivatives by $O_2(^1\Delta)$ have been studied in micelles, reverse micelles, vesicles and membranes. Quenching rates by oxygen are mostly determined by the diffusion of the oxygen in the dispersion media in small aggregates such as micelles and reverse micelles. Due to differences in the entrance rates, deactivation in sodium dodecyl sulfate micelles and cetyl trimethyl ammonium micelles is faster than in the aqueous phase, while the opposite is observed in AOT/hydrocarbon/water reverse micelles. In larger microphases such as vesicles and membranes, deactivation rates are determined by intrabilayer mobility and concentration. The results obtained in erythrocyte plasma membranes and hepatic microsomes indicate an increased oxygen solubility towards the center of the membrane interior, and imply that lateral diffusion contributes more than transverse diffusion to the oxygen mobility.

Photobleaching rates of anthracene derivatives in microphases are extremely sensitive to the location of the probe. This sensibility is due to gradients in the oxygen concentration and micropolarities inside the microphases. The interplay of these two opposite factors determines the relative reactivity of the substrates considered.

INTRODUCTION

The rate of a bimolecular process in a microheterogeneous solution can be employed to sense the properties of the microphases and/or to determine the solubility, location and mobility of the probes and quenchers in (and between) the different microenvironments. Among the more interesting molecules stands oxygen, due to its relevance in biological processes, either normal, pathological or therapeutical.

The information that can be obtained from bimolecular reactions is, in the first place, determined by whether the process is or not diffusionally controlled. Quenching of excited molecules by ground state $^3\Sigma$ oxygen molecules can be considered as a near diffusion controlled process and, as such, can provide information regarding microviscosities and/or diffusion coefficients. On the other hand, singlet oxygen reactions are rather slow processes whose rates are then determined by the local concentration and the microproperties (polarity, water penetration) of the media where the 1O_2 /substrate encounters take place. Both types of studies can provide then a comprehensive description of oxygen solubilization, distribution and mobility in microheterogeneous systems.

In the present work, we discuss results obtained in the following systems:

- Micelles (sodium dodecyl sulfate (SDS) and cetyltrimethylammonium chloride (CTAC))
- Reverse micelles (AOT, CTAC)
- Vesicles (large and small, di-octadecyldimethylammonium chloride (DODAC))
- Biological membranes (rat erythrocyte ghost membranes (RC) and hepatic microsomes).

The present results are complementary to those previously reported by Turro (refs. 1-3), Rodgers (refs. 4-8), Thomas (ref. 9), Lakowicz (refs. 10,11) and Vanderkooi (ref.12).

Prior to the interpretation of the results, two basic questions must be answered:

- How many oxygen molecules are there in each microphase?

- What is the average distance that an oxygen molecule can travel in the time elapsed between excitation and reaction?

The data required to answer those two questions are compiled in Tables 1 and 2.

Table 1. Mean number of oxygen molecules per microphase (\bar{n}) in air equilibrated solutions.

Microphase	\bar{n}
Micelle	0.02
Reverse micelle (R=30)	0.1
Vesicles (small) bilayer	10
water pool	17
Vesicles (large) bilayer	3×10^3
water pool	8×10^4
Membrane	$\gg 10^3$

Table 2. Mean distance travelled by oxygen (in water) as a function of elapsed time.

Time	Distance (A)
1 nsec	16
100 nsec	160
4 μ sec	10^3

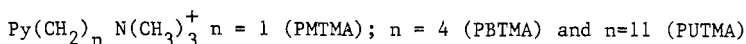
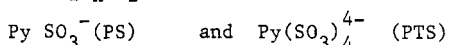
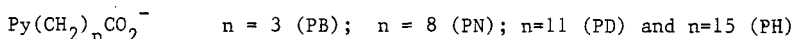
The values of the distance travelled by the oxygen molecule given in Table 2 must be compared with the relevant distances in microheterogeneous systems given in Table 3.

Table 3. Intra and inter microphase distances in microheterogeneous systems.

Parameter	d(A)
Micelle radius	15
Bilayer thickness	40
Vesicle radius (small)	300
(large)	5×10^3
Reverse micelle core (R=30)	50
Distance between micelles (0.1M)	70
Distance between reverse micelles (0.1M)	110
Distance between vesicles, small (2 mM)	2×10^3
large (2 mM)	1.5×10^4

QUENCHING OF EXCITED PYRENE DERIVATIVES BY OXYGEN

Quenching of excited pyrene derivatives by oxygen is a near diffusion controlled process. We have measured the quenching of several pyrene derivatives:



The quenching efficiency was obtained by measuring singlet lifetimes under nitrogen, air and/or oxygen. In all systems considered, the fluorescence decays from ca. 20 nsec after excitation were fitted to monoexponential decays. Pseudo unimolecular quenching constants k_{air} and k_{oxyg} were obtained from eqs. (1) and (2).

$$k_{\text{air}} = \tau_{\text{air}}^{-1} - \tau_{\text{nit}}^{-1} \quad (1)$$

and

$$k_{\text{oxyg}} = \tau_{\text{oxyg}}^{-1} - \tau_{\text{nit}}^{-1} \quad (2)$$

With these definitions, k_{Air}^{-1} and k_{oxyg}^{-1} measure the average time for the first excited probe-oxygen encounter in air-saturated and oxygen-saturated solutions, respectively. Comparison of the values given in Tables 1 to 3 shows that both in micelles and reverse micelles the encounters between micelle-associated probes and oxygen must involve oxygen molecules initially located in the surrounding media. The value of k_{air} and k_{oxyg} will then be determined by the collision rate between oxygen molecules and the micelle (and hence by the size of the micelle and the diffusion of oxygen), and by the probability that an oxygen/micelle encounter be effective in quenching the micelle incorporated probe.

If a simple scheme such as:



is considered, when P stand for the probe, Q for the quencher, W for the aqueous phase and the brackets denote micelle-associated molecules, under the conditions considered (ref.13).

$$k_{Air} = k_+ / (1 + k_- / k_Q) (O_{2w}) \quad (10)$$

where k_+ represents the product of the oxygen/micelles collision rate and the entrance probability. Values of k_{air} and/or k_{oxyg} obtained in micelles are collected in Tables 4 and 5.

Table 4. Quenching by oxygen in SDS and CTAC micelles

Probe	Temp. °C	(τ_{nit})micelle nsec	k_{oxyg} (micelle) 10^6 s^{-1}	k_{oxyg} (water) 10^6 s^{-1}	k_{oxyg} (DODAC) 10^6 s^{-1}
PS	0	141	4.6	4.4	
	22	128(134)	11.0	10	4.2
	50	129	20.3	17	26
PB	0	213	4.1	5	2.5
	22	199	13	10	3.6
	50	182	22	15	30.0
PD	0	198	5.1	-	
	22	193	12.8	-	3.7(a)
	50	160	20	-	
PMTMA	0				
	22	65	13.7	12.8	
	50	43	21.9	18.4	
PBTMA	0				
	22	227	13.6	10.3	
	50	226	21	17	
PUTMA	0				
	22	193	12.8	-	
	50	172	2.1	-	

(a) Data for $\text{Py}(\text{CH}_2)_{15}\text{CO}_2^-$

These data show that all the probes have similar values in aqueous solution, as expected for diffusionally controlled processes. Furthermore, the values obtained in CTAC and SDS solutions are very similar, over all the temperature range, to those measured in aqueous solution. The similarity between the values obtained in water and in micellar solutions, as well as the small dependence with the probe location, is compatible with the above considerations if it is taken into account that the micelles are considerably smaller than the mean distance travelled by the oxygen molecule; hence, the quenching is mostly determined by the diffusion in the surrounding media. Furthermore, given the larger oxygen solubility in the micellar pseudophase than in the surrounding media (ref. 14), incorporation into the micelle must be a very efficient process. The faster rates of quenching observed when the probes are associated to the micelles, particularly at the higher temperatures, result from the large rates of oxygen micelle encounters (ref. 13) and the high efficiency of oxygen incorporation. Eqn. (8) shows that, for small aggregates

for which it can be considered that $k_q \gg k_{air}$, the value of k_{air} in the micelles can become larger than the value in water.

Oxygen quenching in reverse micelles has been studied in AOT/isooctane/water, AOT/dodecane/water, AOT/chloroform/water and CTAC/chloroform/water (Ref. 15). Results obtained in AOT/hydrocarbon/water systems are shown in Table 5.

Table 5. Quenching by Oxygen in AOT/isooctane/water and AOT/dodecane/water systems.

Probe	Solvent	R	k_{air} (10^7sec^{-1})	Isooctane/dodecane
Methylpyrene	Isooctane	-	10	2.7
PUTMA	AOT/Isooct.	1	6.2	2.4
		20	5.1	2.1
BBTMA	Water	-	0.24	
	AOT/Isooct.	1	4.5	1.9
		20	3.6	1.9
PMTMA	Water	-	0.24	
	AOT/Isooct.	1	3.8	2.1
		20	3.0	1.8
PS	Water	-	0.22	
	AOT/Isooct.	1	3.4	1.8
		20	2.3	1.6
PTS	Water	-	0.2	
	AOT/Isooct.	1	0.1	
		25	0.15	

These data show the pseudounimolecular deactivation rate constants in the micellar solutions are, for all the compounds but PTS, intermediate between those obtained in isooctane (methylpyrene as probe) and water. The range of R values considered comprises the region where a "pool" cannot be defined ($R < 8$) and the region of large R values where a distinct water rich core can be considered. The protection afforded by the micelle depends both on the size of the alkyl chain and the charge of the probe. As expected, shorter alkyl chains and similar charge of the probe and surfactant increases the protection as a result of a deeper average location of the pyrene groups. This effect is particularly evidenced for PTS, that, being displaced towards the center of the micelle, is considerably protected from the incoming oxygen. The difference observed in k_{air} values when dodecane and isooctane are the intermicellar solvents emphasize the role of diffusion in the dispersion media. However, it is interesting to note that $(k_{air})_{isooctane} / (k_{air})_{dodecane}$ values are smaller in the micellar solution than in the bulk solvents and that they depend both on the probe considered and the value of R. In particular, the data show that PUTMA presents the largest $(k_{air})_{isooctane} / (k_{air})_{dodecane}$ values as a consequence of its deeper penetration into the hydrocarbon pseudophase.

The restriction imposed by the reverse micelles can be a consequence of a kinetic barrier (i.e. due to the high viscosity of the interface) or the low oxygen solubility in the micellar pseudophase. In this regard, it is interesting to note that, when chloroform is employed as organic solvent, the values of $(k_{air})_{bulk} / (k_{air})_{AOT}$ are smaller than those obtained by employing isooctane (a solvent of similar viscosity) as the dispersion medium (ref.15). This difference can be explained in terms of an easier penetration of oxygen through the interface, likely due to a more favourable oxygen partitioning between the solvent and the surrounding solvent.

Large unilamellar vesicles can incorporate several oxygen molecules in air equilibrated solutions. As such, the quenching can be determined by the intra-bilayer properties and be considerably less conditioned by diffusion of the oxygen molecules in the surrounding media. Quenching by oxygen is then determined by the bilayer properties (Ref.16). The data given in Table 6 also support this view. These data show that all pyrene derivatives are quenched, at low temperatures, slower than when they are dissolved in the aqueous solution, a result that reflects the low solubility and/or mobility of oxygen under these conditions. On the other hand, at temperatures above the bilayer phase transition, quenching by oxygen is considerably faster than in the aqueous solution, due to the higher intravesicular

oxygen concentration. These types of experiments can then provide insight into the capacity of the oxygen molecule to reach different parts of the bilayer. The results of Table 4 would indicate that no substantial differences are observed between the surface (where PS must be locate) and more inner parts of the bilayer (like those where the pyrene group of pyrene hexadecanoic acid is located).

Results obtained in studies of the quenching of probes incorporated to RC (Ref.17) and microsomes by oxygen are presented in Table 6.

Table 6. Pseudounimolecular quenching by oxygen of probes incorporated to erythrocyte ghost membranes and hepatic microsomes at 37°C

Probe	(τ _{nit}) _{RC}	(k _{oxyg}) _{RC}	(k _{oxyg}) _{micr.}	(k _{oxyg.}) _{buffer}
PMTMA	76	9.0	14	18
PBTMA	97	16	15	16
PUTMA	206	20.5	19	--
PB	125	14.5	--	16
PD	201	16	--	--
PH	215	20	--	--

The data of Table 6 show that oxygen easily reaches all parts of the membranes, both in RC and microsomes. The similarity between the values obtained in buffer and in the membranes results from a compensation of a lower mobility and higher solubility in the bilayers. This is also supported by the considerably larger sensitivity of the intra membrane quenching to changes in temperature (ref. 17). An important conclusion from the data obtained in both membranes is that the pseudounimolecular quenching rate constants increase when the length of the probe alkyl chain increases. These results indicate an increased oxygen solubility/mobility towards the center of the membrane interior and imply that lateral diffusion must contribute heavily to the oxygen motion in the membrane. A relevant point to be considered in the interpretation of these results is that, due to the large average distances travelled by the oxygen molecules prior to a probe/oxygen encounter, the velocity of the process is influenced by the microviscosity of large parts of the membrane and not only by the properties of the probe microenvironment. In this sense, quenching experiments provide information different from that derived from fluorescence depolarization experiments.

SINGLET OXYGEN PROCESSES

The photobleaching of an anthracene derivative (A) by singlet oxygen generated by a sensitizer under steady state irradiation can be interpreted in terms of a kinetic scheme similar to that proposed by Rodgers and Lee (ref.18):



with $(k+k') \gg (k_A(A(w)) + k'_A(A(\text{lip})))$, where W and lip stand for the aqueous and lipidic pseudophases, respectively (ref. 19).

Under steady state conditions, in each differential volume dV ,

$$-d(A)/dt = k_A ({}^1O_2)(A) \quad (17)$$

and over all the solution

$$-(dA/dt)_{av} = \frac{1}{V} \int k_A (^1O_2) (A) dV \quad (18)$$

The pseudo unimolecular bleaching constant, defined by

$$k_{exp} = -(d(A)/dt)_{av} / (A)_{Anal} \quad (19)$$

where $(A)_{Anal}$ is the analytical substrate concentration, will be given by

$$k_{exp} = \frac{\int k_A (^1O_2) (A) dV}{(A)_{Anal}} \quad (20)$$

and will be determined by the spatial distribution of (A) and $(^1O_2)$ and the k_A values in each dV . The $(^1O_2)$ concentration will be determined, in a given system, by its generation rate. Also, in microheterogeneous systems, the 1O_2 steady state concentration can depend on the 1O_2 locus of generation. Comparison of the data given in Tables 2 and 3 indicates that only in large vesicle solutions will the site of 1O_2 generation be relevant. In these systems, 1O_2 generated in one vesicle cannot reach other vesicles, and extravascular generated 1O_2 can not maintain similar steady state concentrations in the extra and intra vesicular aqueous solutions (vide infra). For all the other systems, it can be considered that, irrespective of the 1O_2 generation site, the equilibrium depicted by Eqn(2) can be assumed over all the solution.

If (A) is located in a singlet microenvironment

$$k_{exp} = k_A (^1O_2) \quad (21)$$

with k_A and $(^1O_2)$ defined at the probe location. Evaluation of k_{exp} can provide then information regarding the microproperties of the media (through k_A) and/or the local $(^1O_2)$ concentration). However, the product $k_A (^1O_2)$ can not be separated without extra assumptions and, hence, extreme care must be exercised in the interpretation of the results.

If a two pseudophase model is assumed, then one obtains

$$k_{exp} = (^1O_2)_{solv} \cdot (k_{mic} f_{mic} \alpha + (1-f_{mic}) k_{solv}) \quad (22)$$

where α is defined by

$$\alpha = (^1O_2)_{mic} / (^1O_2)_{solv} \quad (23)$$

and f is the fraction of microphase associated probe, related to the probe partition constant (K) through

$$K = \frac{f_{mic}}{(1-f_{mic})} \times \frac{V_{solv}}{V_{mic}} \quad (24)$$

Results obtained in homogeneous systems (ref. 20), SDS and CTAB micelles and AOT reverse micelles (ref. 21) are collected in Tables 7 and 8.

Table 7. Solvent effect on 1O_2 reactions with anthracene derivatives

Probe	Solvent	$k(10^7 \text{ M}^{-1} \text{ sec}^{-1})$
DMA ^a	Benzene	2.5
	Dichloromethane	2.7
	Ethanol	4.6
	Methanol	6.9
	Methanol:w (4:1)	20
	Ethanol:W (1:1)	20
MA ^b	Benzene	0.23
	Ethanol	0.2
	Methanol	0.2
	Ethanol:W (1:1)	1.7
	Water	9.6

^a9,10-dimethyl anthracene; ^b9-methyl anthracene

Table 8. Singlet oxygen reactions in micellar solutions

Probe	Micelle	K _A K ₂	(k _A) _{Mic} / (k _A) ^a (ethanol:w)
DMA	SDS	15	0.27
	CTAB	20	0.25
MA	SDS	4.9	1.0
	CTAB	5.7	0.83
HMA ^b	SDS	1.3	0.58
	CTAB	1.8	0.58
Ac ^{-c}	CTAB	0.74	0.46

^a(k_A)_{Mic} obtained by taking K₂ values from ref. 8.

^b9-hydroxymethyl anthracene

^c9-anthracene carboxylic acid

Comparison of the data given in Tables 7 and 8 shows that incorporation of MA to both SDS and CTAB micelles reduces its rate of reaction with ¹O₂, relative to that expected for the probe in the aqueous solution. This result, which is the opposite of that expected in terms of the higher intramicellar ¹O₂ concentration, can be explained in terms of the strong dependence of the interaction rate with the solution water content. If this factor is considered, the values of k_A derived are very similar to those obtained in ethanol/water mixtures. However, there exist noticeable differences among the different compounds that can be rationalized in terms of their different intramicellar locations. Exposition of the probe to the aqueous pseudophase will noticeably increase its specific rate constant but will, possibly, decrease the local ¹O₂ concentration. The interplay of these two factors will determine the photobleaching rate. Similar arguments can explain results obtained in reverse micelles (ref. 21). In these systems, by applying kinetic treatment based in Eqns. (22) and (24), Rubio and Lissi have shown that AOT reverse micelles strongly catalyze the photobleaching of 9-anthracene methanol, in spite of the decreased concentration of ¹O₂ in the reverse micelles. This catalysis is a consequence of the very high dependence of the interaction rate on the polarity of the microenvironment.

Extensive studies of the reactivity of anthracene derivatives incorporated into vesicles towards singlet oxygen have been carried out by Encinas et al. (ref. 19). Incorporation of the substrates into DODAC vesicles decreases their consumption rates. The effect depends on both the substrate characteristics and the vesicle size, the most pronounced decreases being observed for those substrates for which deep incorporation of the anthryl group into the bilayer could be expected, i.e., DMA and 3-(9-anthryl)propionic acid. For these substrates, the reactivity is nearly two times smaller in the large than in the small vesicles. By applying a two pseudophase formalism, it is possible to evaluate the substrate distribution between the vesicles and the aqueous solution. For MA and HMA, the partition constant are nearly ten times smaller in the large vesicles than in the smaller vesicles. These results where obtained with the dyes solubilized in the whole aqueous solution, and hence homogeneous ¹O₂ concentrations can be assumed over each pseudophase. Results aimed to estimate the ability of the ¹O₂ to diffuse through the vesicles were carried out by producing it outside the vesicles and incorporating the substrate (ethyl dimethyl 3-(9-anthracene)propyl ammonium bromide in to the inner pool of the vesicles. The bleaching rates under these conditions, relative to that obtained in aqueous solution, are given in Table 9.

Table 9. Effect of ethyl dimethyl 3-(9-anthracene)propyl ammonium bromide incorporation into the vesicle inner pool on its reactivity towards ¹O₂

Temperature °C	k _{vesicle} /k _{aqueous}
7	0.06
13	0.105
24	0.24
32.5	0.34

These results indicate that, under these conditions, the steady state concentration in the intravesicular water pool is considerably less than that in the external aqueous pseudophase. The rather large effect of temperature most likely reflects the increase in ¹O₂ permeation rate through the bilayer.

Acknowledgements

This work was carried out with the financial support of FONDECYT (035/88).

REFERENCES

1. M.W. Geiger and N.J. Turro, Photochem. Photobiol. **22**, 273-276 (1975).
2. M.W. Geiger and N.J. Turro, Photochem. Photobiol. **26**, 221-224 (1977).
3. N.J. Turro, M. Aikawa and A. Yekta, Chem. Phys. Letters, **64**, 473-478 (1979).
4. A.A. Gorman, G. Lovering and M.A.J. Rodgers, Photochem. Photobiol. **23**, 399-403 (1976).
5. A.A. Gorman and M.A.J. Rodgers, Chem. Phys. Letters, **55**, 52-54 (1977).
6. B.A. Lindig and M.A.J. Rodgers, Photochem. Photobiol. **33**, 627-634 (1981).
7. M.A. Rodgers and A.L. Bates, Photochem. Photobiol. **35**, 473-477 (1982).
8. P.C. Lee and M.A.J. Rodgers, J. Phys. Chem. **87**, 4894-4898 (1983).
9. M. Wong, I.K. Thomas and M. Gratzel, J. Am. Chem. Soc. **98**, 239 (1976).
10. J.R. Lakowicz "Diffusive transport of oxygen through proteins and membranes quantified by fluorescence quenching", in Hemoglobin and Oxygen Binding, Vol. 1 C, Ho et al. (Eds.) 443-448 (1982).
11. J.R. Lakowicz, J. Biochim. Biophys. Methods **2**, 90-119 (1980).
12. S. Fischkoff and J.M. Vanderkooi, J. Gen. Physiol. **65**, 663-676 (1975).
13. E.A. Lissi, A. Dattoli and E.B. Abuin, Bol. Soc. Chil. Quim. **30**, 37-44 (1985).
14. I.B.C. Matheson and R. Massoudi, J. Amer. Chem. Soc. **102**, 1942-1948 (1980).
15. M. Sáez, E.B. Abuin and E.A. Lissi, Langmuir, **5**, 942-947 (1989).
16. E.B. Abuin, E.A. Lissi, D. Aravena, A. Zanocco and M. Macuer. J. Colloid Interface Sci. **122**, 201-208 (1988).
17. E.A. Lissi and T. Cáceres. J. Bioenerg. and Biom. **21**, 375-385 (1989).
18. M.A.T. Rodgers and P.C. Lee, J. Phys. Chem. **88**, 3480 (1988).
19. M.V. Encinas, E. Lemp and E.A. Lissi, J. Photochem. Photobiol. B: Biology, **3**, 113-122 (1989).
20. M.A. Rubio, L. Araya, E.B. Abuin and E.A. Lissi, An. Asoc. Quim. Argent., **73**, 301-309 (1985).
21. M.A. Rubio and E.A. Lissi, J. Colloid & Int. Sci., **128**, 458-463 (1989).